

Adaptation of Kurganov-Tadmor Numerical Scheme For Applying in Combination With the PISO Method in Numerical Simulation of Flows in a Wide Range of Mach Numbers

Matvey Kraposhin¹, Arina Bovtrikova¹ and Sergei Strijhak²

¹ISP RAS, Moscow, Russian Federation

²HP, Moscow, Russian Federation

os-cfd@yandex.ru, pudjic@mail.ru, strijhak@yandex.ru

Abstract

In this work a hybrid scheme based on the PISO-algorithm and Kurganov-Tadmor's numerical scheme is proposed. This scheme utilizes compressible PISO method for coupling between velocity and pressure and Kurganov-Tadmor scheme for formulation of non-oscillating convective fluxes. Compressible and incompressible regimes of developed model are switched with blending function depending on local Mach and CFL number. A numerical scheme is implemented by means of OpenFOAM ver. 2.3.0 as pisoCentralFoam independent solver. Investigation of the mathematical model was conducted and exemplified by test cases. Proposed scheme can be used for wide range of Mach numbers from 0.01 to 3 or higher. The mesh convergence was analyzed. Comparison of the results with the experimental and analytic data was carried out. The solver was tested in a parallel mode on a computer cluster.

Keywords: compressible flow, numerical schemes, explicit and implicit approach, model validation, parallel computations

1 Introduction

Numerous problems of gas dynamics require modeling of turbulent compressible flows in a wide range of Mach numbers. The possibility of ensuring solution's monotonicity in discontinuities is one of the main criteria of quality estimation of the method during computational modeling of such flows. In resolving practical issues this is achieved by using such special schemes as discontinuity-disintegration scheme (approximate solution of the Riemann's problem), Kurganov-Tadmor's scheme (KT) [1,2], AUSM+ scheme [3,4] etc. Implementations of these schemes in commercial packages as well as in OpenFOAM open source software package of different versions [5,6] made a good showing while resolving problems of viscous and non-viscous liquid flows. The only disadvantage of its using

is the medium's velocity limitation at the lower boundary of applicability range: the minimum Mach number must approach to the transonic conditions. Employing these models for viscous flow simulation with low Mach numbers (< 0.3) is impossible even with decreasing enough the time step to prevent the acoustic Courant criteria to be greater or equal to $1/2$. Such limitations creates several impediments for studies of devices' aerodynamics in marginal conditions with the help of a single model – for example, while changing from the subsonic to the supersonic flow conditions. At the same time there is a range of semi-implicit methods for solving subsonic problems that are successfully employed in industry for high Mach number flows — PISO, SIMPLE and their combinations [10]. The inconvenience of these methods consists in occurrence of numerical oscillations in the regions of flow properties' discontinuities, that take place in high-speed flows — for example, Kurganov-Tadmor scheme and the PISO algorithm are compared in [7]. The solution might be found in hybrid scheme's implementation, for which PISO/SIMPLE algorithms for implicit integration of the mass (1), momentum (2) and energy (3) conservation equations are employed in combination with corresponding schemes for the non-oscillating discretization of the convective terms.

$$\frac{\partial \rho}{\partial t} + \nabla \cdot (\rho \vec{U}) = 0 \quad (1)$$

$$\frac{\partial \rho \vec{U}}{\partial t} + \nabla \cdot (\rho \vec{U} \vec{U}) = \nabla \cdot \Pi + \vec{F}_b \quad (2)$$

$$\frac{\partial \rho e}{\partial t} + \nabla \cdot (\rho \vec{U} e) = \nabla \cdot (\Pi \cdot \vec{U}) + \vec{F}_b \cdot \vec{U} - \nabla \cdot \vec{q} \quad (3)$$

Where ρ - density, \vec{U} — velocity of the medium, \vec{F}_b — the main vector of mass forces, Π — the normal and viscous tension tensor, e — the total energy of the flow (the sum of kinetic and internal energies), \vec{q} — heat flux. According to the Newtonian liquid approach the tension tensor is computed via the strain rate tensor and the pressure's field $\Pi = (-p + \frac{2}{3} \nabla \cdot \vec{U})I + \mu (\nabla \vec{U} + (\nabla \vec{U})^T)$, where p — pressure, I — unitary matrix, μ — dynamic viscosity. The Fourier's law is engaged to calculate the heat flux: $\vec{q} = -\lambda \nabla T$, where T — medium's temperature, λ — heat conductivity. It is assumed that medium is a perfect gas, i. e. $p = \rho \tilde{R} T$, $\tilde{R} = R/M$ - individual gas constant, R — universal gas constant, M — molar mass of the considered gas.

Attempts to develop such hybrid schemes have already been made, for example in [8] it is suggested to use AUSM+ scheme together with the PISO algorithm. Despite the promising results presented in the article, the search of source code implementation of the proposed technique has failed. Moreover, in our opinion, the AUSM+ technique has the following disadvantages: 1) the complexity of implementation, and 2) the presence of adjustable coefficients — model constants. Therefore, we decided to pay attention to Kurganov-Tadmor's scheme (or rather its Kurganov-Noelle-Petrova version, or abbreviated KNP) which on one hand is already explicitly implemented in OpenFOAM package and has been repeatedly tested, and on the other hand it is simple enough to be used as part of a hybrid scheme. Another important feature of this scheme is independence of approximating expressions for the fluxes of physical quantities from the characteristics of the studied system of equations. Thus, there is no need to use solution expansion on characteristics for calculation of flows. The limitation of Kurganov-Tadmor's scheme is the need to maintain the acoustic Courant number less than $1/2$, which leads to understated time steps in the case of low-velocity medium. Furthermore, non-physical “circuital” time oscillations appear when solving subsonic tasks. Our proposed hybrid scheme based on PISO and KT/KNP, on the one hand, meets the requirement on monotonicity, and on the other hand it would allow simulating flow in a wide range of Mach numbers $0 < M < 3$. In this case, simulation in the range of low and very low Mach numbers ($M < 0.5$) would be possible with an acoustic Courant number far exceeding 1. The idea of the method consists in the introduction of a switcher which when approaching to subsonic speed range would switch approximate expressions for fluxes to a standard form used in PISO method:

$$\int_V \nabla \cdot (\vec{U} \Psi) dV = \int_S d\vec{S} \cdot (\vec{U} \Psi) = \sum_f \Psi_f (\vec{U} \cdot \vec{S}_f) = \sum_f \Psi_f \varphi_f \quad (4)$$

Where Ψ — some transferable value, f index — No. of a face of a cell, \vec{S}_f — product of vector of a face normal on its area. Values with f index are interpolated on a surface mesh from volume mesh. To compare the designations of KT/KNP scheme, proposed in [1,2] with standard designations, used in the finite volume method, see Figure 1. P point indicates the center of some control volume for which balances of mass, momentum and energy are considered. In one-dimensional case, point P of this volume has coordinate X_j . Expressions for flows are written for the right boundary of this volume,

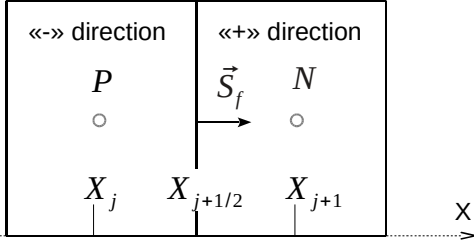


Figure 1. Comparison of finite volume computing molecule in case of unstructured meshes (OpenFOAM) and structured meshes (KT/KNP)

with the normal directed along the X axis from P point to N point, location of face center — $X_{j+1/2}$, location of the a neighboring volume center $N - X_{j+1}$.

In this case, according to KT/KNP [1,2] scheme, flux of field Ψ through the face can be represented as a weighted sum of fluxes in positive and negative directions. In particular, the advective fluxes include not only macroscopic velocity of the medium, but also acoustic speed of disturbances propagation:

$$\Psi(X_{j+1/2})\varphi(X_{j+1/2}) = \frac{a_{j+1/2}^+ f(\Psi_{j+1/2}^-) - a_{j+1/2}^- f(\Psi_{j+1/2}^+)}{a_{j+1/2}^+ - a_{j+1/2}^-} + \frac{a_{j+1/2}^+ a_{j+1/2}^-}{a_{j+1/2}^+ - a_{j+1/2}^-} (\Psi_{j+1/2}^+ - \Psi_{j+1/2}^-) \quad (5)$$

To switch to the designation system used in the finite volume method we introduce the following designation:

$$a_f^{max} = a_{j+1/2}^+, \quad a_f^{min} = a_{j+1/2}^-, \quad \alpha_f^P = \frac{a_f^{max}}{a_f^{max} + a_f^{min}}, \quad \alpha_f^N = \frac{a_f^{min}}{a_f^{max} + a_f^{min}}$$

$$\Psi_f^P = \Psi_{j+1/2}^-, \quad \Psi_f^N = \Psi_{j+1/2}^+, \quad \varphi_f^P = f(\Psi_{j+1/2}^-), \quad \varphi_f^N = f(\Psi_{j+1/2}^+), \quad \omega_f = \alpha_f^P a_f^{min}$$

Then, the expression for the calculation of convective flux of Ψ value through the face takes the form of [6]:

$$\Psi_f \varphi_f = \alpha_f^P \varphi_f^P \Psi_f^P + \alpha_f^N \varphi_f^N \Psi_f^N - \omega_f (\Psi_f^P - \Psi_f^N) \quad (6)$$

or after transposition of terms

$$\Psi_f \varphi_f = \Psi_f^P (\alpha_f^P \varphi_f^P + \alpha_f^P a_f^{min}) + \Psi_f^N (\alpha_f^N \varphi_f^N - \alpha_f^P a_f^{min}) \quad (7)$$

Here, the superscript indicates the cell, which value is used for interpolation on the face f , if P then the cell is used, with respect to which the normal is external, if N then the cell is used, with respect to which the normal is internal.

To calculate the coefficients α_f^P, α_f^N we use volume fluxes a_f^{max} and a_f^{min} , relative to local sound speed in the medium:

$$a_f^{max} = \max(c_f^P |\vec{S}_f| + \varphi_f^P, c_f^N |\vec{S}_f| + \varphi_f^N)$$

$$a_f^{min} = -\min(-c_f^P |\vec{S}_f| + \varphi_f^P, -c_f^N |\vec{S}_f| + \varphi_f^N) \quad (8)$$

$$c_f^P = \sqrt{\gamma_f^P \bar{R} T_f^P}, \quad c_f^N = \sqrt{\gamma_f^N \bar{R} T_f^N}$$

Where $\gamma = Cp/Cv$ — adiabatic number of gas (heat capacities ratio).

To calculate the values of Ψ_f^P and Ψ_f^N on the face we use interpolation schemes of the second order with a limiter. Generally, we use symmetric TVD schemes — vanLeer, Minmod, vanAlbad, etc. as a limiter.

2 Description of proposed hybrid scheme

As already mentioned, KT/KNP scheme implemented in OpenFOAM is explicit, which makes it unsuitable for the study of flows with small numbers $M < 0.5$. In order to achieve the possibility of simulating flows in this range, including those with small time steps, we have proposed a hybrid scheme, which allows combining properties of PISO/SIMPLE and KT/KNP algorithms using a switch function. The idea of a hybrid scheme is as follows:

- 1) Formulate mass fluxes in the form (7) according to the KT/KNP schemes;
- 2) Introduce some mixing function which allows “switching” between incompressible and compressible flux formulations;
- 3) Write the equation of conservation of mass and momentum and energy in semidiscrete form suitable for derivation of the pressure equation;
- 4) Apply PISO/SIMPLE method to discretize equations in which the convective terms are approximated by means of “switcher” function and KT/KNP scheme (7).

The use of this approach not only greatly simplifies the implementation of schemes in OpenFOAM, but also allows accounting turbulence with built-in library functions. To mix subsonic and supersonic formulations, write the mass fluxes using the mixing function κ_f :

$$\begin{aligned} \Phi_f^P &= \kappa_f \rho_f^P (\alpha_f^P \phi_f^P + \alpha_f^P a_f^{min}) \\ \Phi_f^N &= (1 - \kappa_f) \rho_f^P (\alpha_f^P \phi_f^P + \alpha_f^P a_f^{min}) + \rho_f^N (\alpha_f^N \phi_f^N - \alpha_f^P a_f^{min}) \end{aligned} \quad (9)$$

When using the KT scheme instead of KNP, the form of terms will change, but the concept will remain. With the increasing influence of compressibility, switch κ_f shall strive for 1, and then Φ_f^N and Φ_f^P - fluxes degenerate into mass fluxes, calculated based on KT/KNP scheme. Instead, when κ_f approaching to 0, flux Φ_f^N strives for the flux formulation in an incompressible approach, and flux Φ_f^P strives for 0.

Based on the above description of the proposed hybrid scheme we can propose the following form of κ_f function:

$$\kappa_f = \min \left(\frac{M_f}{CFL}, 1 \right) \quad (10)$$

Where M_f - local Mach number at face f , CFL - Courant-Friedrich-Levy criterion at face f .

Finite volume discretization of convective and diffusive terms of equation (2) leads to the system of algebraic linear equations [10] for each component of the flow velocity. For such semi-discrete approximation standard notation is used (for example, like in [10]):

$$A \vec{U} = \frac{\vec{H}}{V} - \nabla p \quad (11)$$

Where A — diagonal coefficients of the matrix, \vec{H} — total contribution of the off-diagonal matrix coefficients, and V — volumes of cells. To get the final equation for the pressure, expression (11) must be substituted into continuity equation.

The continuity equation (1) in the discrete form with convective fluxes substituted from (9):

$$\begin{aligned} \frac{\delta\rho}{\delta t} + \frac{1}{V} \sum_f (\Phi_f^P + \Phi_f^N) \\ = \frac{\delta\rho}{\delta t} + \frac{1}{V} \sum_f (\rho_f^P (\alpha_f^P \varphi_f^P + \alpha_f^P a_f^{min}) + \rho_f^N (\alpha_f^N \varphi_f^N - \alpha_f^P a_f^{min})) = 0 \end{aligned} \quad (12)$$

Where $\delta/\delta t$ — operator of discrete partial differentiation with respect to time. Fluxes φ_f^N and φ_f^P are calculated by the interpolated velocity obtained in accordance with semidiscrete expression (11) in the control volume centers N and P, as it is done in the standard method of PISO or SIMPLE

$$\begin{aligned} \varphi_f^N &= \left(\frac{1\vec{H}}{V A} \right)_f^N \cdot \vec{S}_f - \left(\frac{\nabla p}{A} \right)_f^N \cdot \vec{S}_f \\ \varphi_f^P &= \left(\frac{1\vec{H}}{V A} \right)_f^P \cdot \vec{S}_f - \left(\frac{\nabla p}{A} \right)_f^P \cdot \vec{S}_f \end{aligned} \quad (13)$$

Substituting the expression for convective flows (13) and the perfect gas equation of state in discrete continuity equation, we obtain the equation for the pressure generated taking into account KT/KNP scheme:

$$\begin{aligned} \frac{\delta\psi p}{\delta t} + \\ \frac{1}{V} \sum_f (\psi p)_f^N \left(\alpha_f^N \left[\left(\frac{1\vec{H}}{V A} \right)_f^N \cdot \vec{S}_f - \left(\frac{\nabla p}{A} \right)_f^N \cdot \vec{S}_f \right] - \alpha_f^P a_f^{min} \right) + \\ \frac{1}{V} \sum_f (\psi p)_f^P \left(\alpha_f^P \left[\left(\frac{1\vec{H}}{V A} \right)_f^P \cdot \vec{S}_f - \left(\frac{\nabla p}{A} \right)_f^P \cdot \vec{S}_f \right] + \alpha_f^P a_f^{min} \right) = 0 \end{aligned} \quad (14)$$

Here $\psi = 1/(\tilde{R}T)$ — gas compressibility.

This equation is non-linear with respect to the pressure due to: 1) Presence of pressure as a coefficient in diffusion terms; 2) Dependency of and terms on unknown and fluxes, which themselves depend on pressure. Thus, to solve it we need linearization. The practice of testing of the proposed scheme on various models has showed that the use of the values of these coefficients from the previous step with the technique of internal iterations is sufficient to achieve the required accuracy of the results and to ensure the mesh convergence. Approximation of convective transport of other variables (velocity and total energy) is performed by means of fluxes (9), which are obtained by solving the equation for the pressure (14). As for the rest, integration algorithm of system of equations of fluid corresponds to well-known methods of operators splitting class — PISO, SIMPLE, etc. The described hybrid scheme has been implemented by means of the finite volume library OpenFOAM 2.3.0 as an application – pisoCentralFoam “solver”, and tested for a wide range of Ma and Re numbers.

3 Scheme validation

Developed numerical scheme has been tested for a set of cases with Mach number from 0.03 to 3 and Re numbers from 100 to 100000.

3.1 Wave propagation in channel of constant area (Shock tube problem)

Shock wave propagation in a cylindrical channel was investigated. The wave is generated by the expansion of compressed air of high pressure and temperature to the region of low pressure and

temperature. The computational domain of the problem is 3D cylinder. Gas in both right and left zones is the air. This one-dimensional problem has its analytical solution in Anderson, Jr, John D. «Modern Compressible Flow: With Historical Perspective». At the initial time point the regions of different pressures are separated with a diaphragm. After the diaphragm's rupture a compressive wave begins its propagation in the low pressure direction, the same for an exhaustion wave in the high pressure direction. Depending on the left and right pressure ratio the gas stream can be subsonic or supersonic - see Table 1. The both cases were considered during testing of pisoCentralFoam solver.

Table 1. Initial conditions for shock tube problem

| Region | Subsonic flow | | Supersonic flow | |
|-----------------------------|------------------------|----------------|------------------------|----------------|
| | Pressure, Pa | Temperature, K | Pressure, Pa | Temperature, K |
| Left part of the diaphragm | $P_4=6,897 \cdot 10^4$ | $T_4=288,89$ | $P_4=6,897 \cdot 10^4$ | $T_4=288,89$ |
| Right part of the diaphragm | $P_1=5,897 \cdot 10^4$ | $T_1=288,89$ | $P_1=6,897 \cdot 10^3$ | $T_1=231,11$ |

The computation was conducted up to the moment $t=0.00025s$. The results show that distribution of the pressure in cross-section is uniform in 2D in 3D cases, and the solution of the problem does not depend on dimension. Comparison of one-dimensional case results with the analytical solution is given in Figure 2 and Figure 3. These figures show, that the numerical solution, obtained with developed model is in good agreement with analytical solution and does not oscillate.

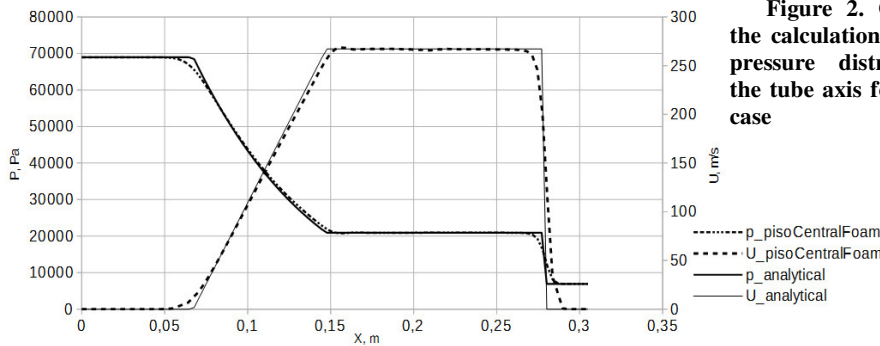


Figure 2. Comparison of the calculation and analytical pressure distribution along the tube axis for the subsonic case

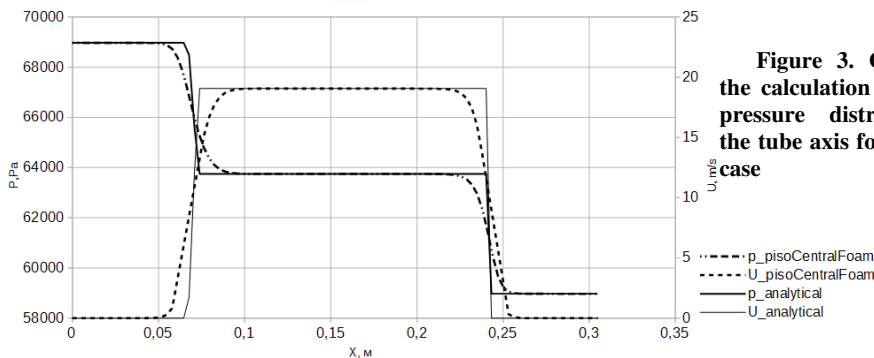


Figure 3. Comparison of the calculation and analytical pressure distribution along the tube axis for the transonic case

3.2 Backward facing step

For the third test case the classical problem from the theory of detached flow – two-dimensional flow over the backward-facing step – was considered. The picture of the flow is presented in Figure 5. The flow expands while passing through the edge and forms the fan of waves of exhaustion. An obstacle in the form of horizontal surface determines the viscous flow separation. The reattachment leads to λ -shaped shock wave's formation.

Information from [11] was used as reference data. Mach number of the free stream flow $M=2.5$. The actuating medium is dry air, $k-\omega$ SST turbulence model was used. Static pressure of the incident flow is 13316.6 Pa, the stagnation pressure is 227.5kPa and the stagnation temperature is 344K.

The mesh was constructed with 3 rectangular blocks. For all the solid walls a no-slip boundary condition was assigned, k and ω were approximated with wall functions. The results were compared to the experimental data from [12], and with computational data from PARC, WIND and ANSYS Fluid Dynamics codes. The computation was stopped after 0.06 s, when the flow became steady.

In order to qualitatively estimate correctness of resolution of supersonic flow spatial characteristics in the presence of shock we made comparison with experimental and numerical data. Figure 5 shows

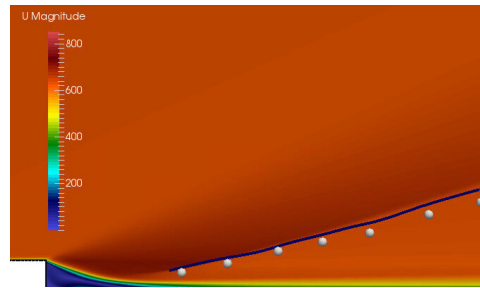


Figure 5. Flow pattern and comparison of the reattachment shock location for backward facing step case. Experimental position of shock marked with gray points, numerical position of shock, obtained with code PARC[12] shown with blue line

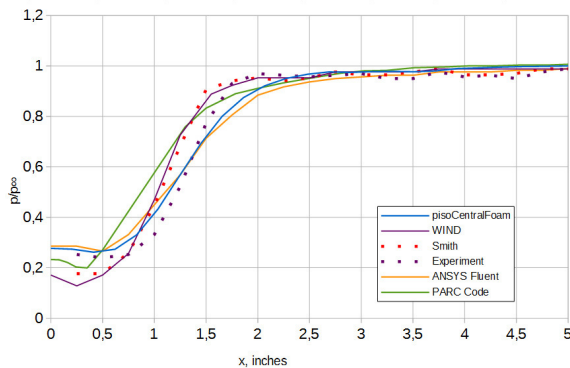


Figure 6. Comparison of pressure distribution

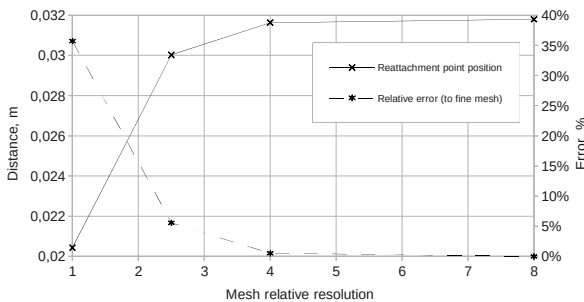


Figure 7. Mesh convergence of the developed numerical scheme for the case of backward step

flow structure, obtained with developed model and its comparison with experimental and numerical position of shock from [12] and numerical position of shock, obtained in PARC code [13]. As it can be seen from picture, our prediction of shock position both in good agreement with side numerical results and experimental data.

Comparison between pressure distribution obtained in this work and experimental and numerical data from other authors behind the step is shown in 6.

Pressure is normalized with the static inlet pressure, and the coordinate in inches is measured from the step. As we can see, pisoCentralFoam performs better with reference experimental and numerical data from [11], ANSYS Fluid Dynamics Guide. At the same time the curve, obtained with developed model, is slightly different from the data in the report [12] and from numerical results of WIND and PARC codes [13]. The pressure in the stagnation region is over-predicted relatively to these sources. We need to mention that the original reference experimental pressure

distribution from [11] hasn't been found in report [12]. Result of conducted mesh convergence survey is presented in Figure 7. It is seen from this Fig. 7 that developed scheme is 2nd order in space, and numerical solution tends to an accurate one after refining mesh with factor 4 in each direction in the region of separation.

3.3 Flow in a supersonic nozzle with a normal shock

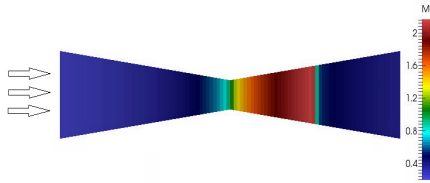
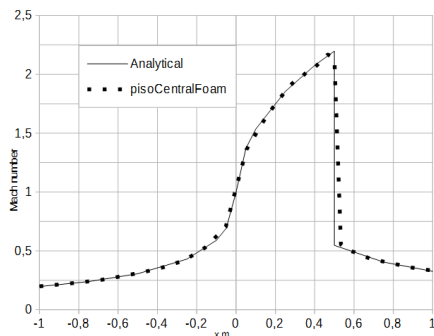


Figure 8. Steady flow over the nozzle - Mach number distribution along axis of nozzle



The wind tunnel is 1 unit length and 3 units long.

Figure 9. Comparison of Mach number's distribution along the nozzle's length

at initial time point on all space of the channel. The case uses a gas with $\gamma = 1.4$ and is initialized with $p=1, T=1$ and Mach 3. For simplicity, we set specific gas constant $R=0.714$, so that the speed of sound $c=1$ and the flow velocity $u=(3,0,0)$ corresponds directly to the Mach number. The calculation was performed until $T=4$ sec time. We compared the position of λ -shaped shock wave's "leg" and the presence/absence of Kelvin-Helmholtz instability observed in many studies during reproduction of the case. Given the correct discretization is present at $T=4$ sec moment of time, the position of λ -shaped shock wave's "leg" shall fall within the leading ledge ($X=60$ cm). This case was used to test the scalability of the model and investigation of the mesh convergence with respect to time and space. The results of the mesh convergence are provided only for medium, refined and very fine meshes. Parameters of coarse mesh are for reference only.

Based on the calculations it becomes clear that regardless of the degree of refining of the estimated mesh the position of λ -shaped shock wave's corresponds to the position of the step (see Figure 10). In this case, when using the first-order scheme with respect to time, Kelvin-Helmholtz instability starts to appear only on the finest mesh (4 million cells), while the use of the second-order approximation scheme with respect to time allows reproducing this effect on a more coarse mesh as well (1 million

The problem of a flow over the simplest supersonic nozzle was considered. The nozzle geometry was modeled with a combination of two truncated cones (Figure 8). The initial data correspond to the calculation case from [11]. The results were compared to the analytical solution based on the laws of isotropic flow of an ideal gas and the theory of normal shock [16], as well as to the results of simulation in ANSYS Fluid Dynamics.

The ratio of inlet and outlet cross-sections to the throat cross-section is equal to 3. As it is seen on the Figure 9, the analytical and computational Mach number distributions almost coincide, except some difference in the shock area, which could be explained with the diffusion of the scheme. The error value is less than 6 %.

3.4 Forward-facing step problem with supersonic flow

The supersonic flow of ideal inviscid gas is considered in the wind tunnel with a sharp narrowing. The step is 0.2 units high and is located 0.6 units from the inlet on the left. The flow in tunnel is assumed to be two-dimensional. The velocity, pressure and temperature are distributed uniformly

cells) — see Figure 10. Investigation of solver's scalability has showed satisfactory acceleration on 1 million cells mesh and superlinear acceleration for 4 million cells mesh – see Figure 11.



Figure 10. Comparison of flow patterns (density) for the case calculated with the first order of approximation with respect to time on the finest mesh, and for the case calculated with the second order of approximation

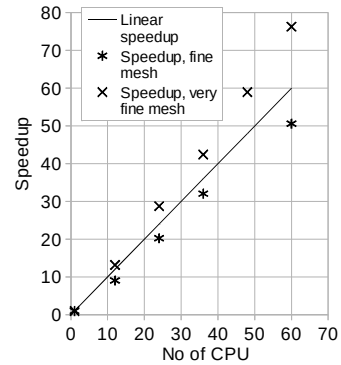


Figure 11. Comparison of scalability of the developed solver for 1 million cells mesh and 4 million cells mesh

3.5 Subsonic laminar viscous flow in the channel of round cross section

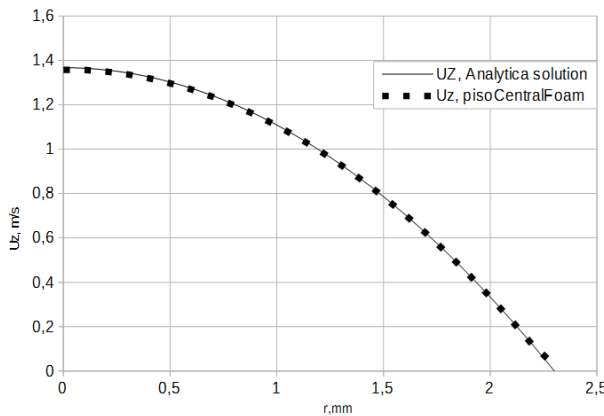


Figure 12. The comparison of analytical and calculated distributions of $U_z(r)$ in the channel

channel for laminar profile at the outlet. The results of comparison of analytical solutions [16] for laminar profile at the outlet of the computational domain and numerical solution, obtained by means of this model are shown in Figure 12. The Mach number amounted to 0.002. The calculation was conducted with a time step of 30-40 μ s, which corresponds to the acoustic Courant number of ~ 1300 .

By means of this calculation case we check the validity of reproduction of diffusion terms in momentum conservation equation (strain tensor) at low Mach numbers. As for this case the analytical solution is known, it is possible to assess the accurate quantity of error between the exact and approximate solutions. For the formulation of the task, it is assumed that the number $Re=200$, viscosity is calculated from the physical data defined in the formulation of initial and boundary conditions.

The velocity profile at the inlet is uniform. The computational domain is a sector of a cylindrical channel with a length substantially greater than the diameter of the

4 Conclusions

We have proposed and implemented a hybrid semi-implicit model of viscous perfect gas flow with the field of applicability in a wide range of Mach numbers – from deep incompressible flow ($Ma < 0.1$) to

supersonic flow ($M > 3$). The developed model is based on the adaptation of the explicit Kurganov-Tadmor scheme (and its KNP modification) for the use as part of the PISO operators splitting method. The advantage of the scheme is the combination of the best features of these approaches in one model: 1) Simple implementation; 2) Monotonicity of solution; 3) The possibility of sustainable numerical simulation of subsonic flows with a small time step; 4) Automatic switching between the subsonic, transonic and supersonic schemes; 6) Support of existing OpenFOAM functional library. The model was tested in compressible and incompressible approximation for 1D, 2D and 3D flows in a wide range of Reynolds and Mach numbers. The obtained results show a good degree of coincidence with the analytical functions and experimental data. Mesh convergence of the method is demonstrated with respect to space and time. It is shown that the scheme achieves the 2nd order of approximation. We have shown the possibilities of the use of scheme in parallel mode. Testing was performed on 1 million and 4 million cells meshes, and the number of cores from 1 to 60. We have shown the possibility of nearly linear acceleration even with a small ratio of the number of cells on the computational core.

This research is funded by The Ministry of Education and Science of Russia (RFMEFI60714X0090, grant number 14.607.21.0090)

References

- [1] A. Kurganov, E. Tadmor. «New High-Resolution Central Schemes for Nonlinear Conservation Laws and Convection–Diffusion Equations» // *Journal of Computational Physics* 160, 241–282 (2000), doi:10.1006/jcph.2000.6459
- [2] A. Kurganov, S. Noelle, G. Petrova. «Semi-discrete central-upwind schemes for hyperbolic conservation laws and Hamilton–Jacobi equations» // *SIAM Journal on Scientific Computing* 2001; 23:707–740
- [3] M.S. Liou, C.J. Steffen Jr. «A new flux splitting scheme» // *J. Comput. Phys.*, 107 (1) (1993), pp. 23–39
- [4] M.S. Liou «A sequel to AUSM: AUSM+» // *J. Comput. Phys.*, 129 (2) (1996), pp. 364–382
- [5] C. J. Greenshields, H. G. Weller, L. Gasparini, J. M. Reese «Implementation of semi-discrete, non-staggered central schemes in a colocated, polyhedral, finite volume framework, for high-speed viscous flows» // *Int. J. Numer. Meth. Fluids* 2010; 63:1–21, DOI: 10.1002/flid.2069
- [6] S. Chuna, S. Fengxianb, X. Xinlina «Analysis on capabilities of density-based solvers within OpenFOAM to distinguish aerothermal variables in diffusion boundary layer» // *Chinese Journal of Aeronautics*, Volume 26, Issue 6, December 2013, Pages 1370–1379, <http://dx.doi.org/10.1016/j.cja.2013.10.003>
- [7] L. F. Gutiérrez Marcanton, J. P. Tamagno, S. A. Elaskar «HIGH SPEED FLOW SIMULATION USING OPENFOAM» // *Mecánica Computacional Vol XXXI*, págs. 2939-2959 (artículo completo), Salta, Argentina, 13-16 Noviembre 2012
- [8] C. M. Xisto, J. C. Páscoa, P. J. Oliveira and D. A. Nicolini «A hybrid pressure–density-based algorithm for the Euler equations at all Mach number regimes» // *Int. J. Numer. Meth. Fluids* (2011), DOI: 10.1002/flid.2722
- [9] P. Balachandran "Fundamentals of compressible fluid dynamics" // PHI Learning Pvt. Ltd., 2006
- [10] J. H. Ferziger, M. Peric "Computational Methods for Fluid Dynamics" // 3rd edition, Berlin; Heidelberg; New York; Barcelona; Hong Kong; London; Milan; Paris; Tokyo: Springer, 2002
- [11] ANSYS Fluid Dynamics Verification Manual, Release 15.0, 2013.
- [12] H. E. Smith «The Flow Field and Heat Transfer Downstream of a Rearward Facing Step in Supersonic Flow» // Technical report ARL 67-0056. ARL, Ohio, 1967 (Mar.)
- [13] G. D. Garrard, W.J. Phares. «Calibration of the PARC Program for Propulsion-Type flows», 1991
- [14] C. Liang. «High-order accurate simulation of low-Mach laminar flow past two side-by-side cylinders with Spectral Difference method» // Report ACL 2008-4 Aerospace Computing Laboratory, Aeronautics and Astronautics, Stanford University, May 2008
- [15] X. Liu, «Wind loads on multiple cylinders arranged in tandem with effects of turbulence and surface roughness» // Master thesis, Department of Civil and Environmental Engineering, Louisiana State University, 2003
- [16] F. M. White. «Fluid Mechanics» // 3rd Edition. McGraw-Hill Book Co., New York, NY. 158531. 1994.